On the optical study of Pb additive Se-Te-Ge nano-crystalline quaternary alloys

NEHA SHARMA[a], BALBIR SINGH PATIAL[b,*], PANKAJ SHARMA[c], NAGESH THAKUR[a]
[a]*Department of Physics, H.P. University Summer Hill Shimla, H.P.-171 005 India*
[b]*State Project Directorate, Rashtriya Uchchatar Shiksha Abhiyan (RUSA), Directorate of Higher Education, Shimla, (H.P.) 171001 India*
[c]*Department of Physics, Jaypee University of Information Technology, Waknaghat, H.P.-173215, India*

In the present study, chalcogenide thin films for different compositions $(Se_{80}Te_{20})_{94-x}Ge_6Pb_x$ (x = 0, 2, 4 and 6) were prepared by thermal evaporation technique. Optical transmission spectra were taken in the wavelength ranges from 500-2600 nm. By using the maxima and minima of the interference fringes, optical constants and thickness of the films were derived. Dispersion of refractive index was analyzed using the single-oscillator Wemple and DiDomenico model. Optical band gap (E_g) for non-direct transition was estimated by the Tauc relation. E_g was found to decrease with the increase in lead content. It was found that with the increase in lead concentration, the refractive index (n), absorption coefficient (α), extinction coefficient (k), optical conductivity (σ), real (ε_r) and imaginary part (ε_i) of dielectric constant increases. We also compared the value of static refractive index (n_0) obtained by WDD (Wemple and DiDomenico) model and by Cauchy's dispersion relation, found that these two values were not in consonance to each other.

(Received November 26, 2017; accepted August 9, 2018)

Keywords: Thin films, Optical constants, Nano-chalcogenide

1. Introduction

Chalcogenide nano-materials have been studied in the past few years because of their size dependent properties and their unique physical and chemical properties. These unique properties of nano structured materials have created the possibilities of using them in optical imaging, infrared optics, optical recording and optical communications [1-4]. Still nano particles of chalcogenides were not well studied and a few work has been done in this direction by various researchers [5-6]. Therefore, there was a lot of scope for the study of these materials in a nano range.

It is known that binary and ternary chalcogenides have some drawbacks like low thermal stability, low crystallization temperature and aging effects [7-8]. The selection of Se was due to its large glass forming ability and commercial applications in many industrial fields. Se-Te based was preferred because of higher photosensitivity. The addition of third element further increases the possibility in the variation of properties [9]. Addition of Ge increases the degree of cross-linking and also increases its thermal stability. Lead chalcogenide is the basic material of modern infrared optoelectronics and it is the heaviest atom which provides compactness to the compound material. In present year, there has been an interest in Pb chalcogenides due to its technological importance in crystalline and nanocrystalline forms, detectors of infrared radiation, photoresistors, lasers, solar cells, optoelectronic devices, thermoelectric devices and more recently as infrared emitters and solar control coating [10-14].

In the present study, the optical characterization of newly prepared thin films of $(Se_{80}Te_{20})_{94-x}Ge_6Pb_x$ (x = 0, 2, 4 and 6) is reported and discussed. Transmission spectra is used to determine the optical constants such as refractive index (n), absorption coefficient (α), extinction coefficient (k), optical conductivity (σ), real (ε_r) and imaginary part (ε_i) of dielectric constant in the UV-Vis-NIR region [15].

2. Experimental details

The bulk $(Se_{80}Te_{20})_{94-x}Ge_6Pb_x$ (x = 0, 2, 4 and 6) quaternary alloys were prepared by melt quenching technique. Materials were weighed according to their atomic percentages (99.999%) and sealed in quartz ampoule under a vacuum of 10^{-5} mbar. The sealed ampoules were then heated to a temperature of 1000°C for 10 hours to make the melt homogenous. The materials in the ampoules were in molten state and then quenched in to ice-cold water immediately after taking them out from the furnace. Nano-crystalline nature of the quaternary samples was recognized using the X-ray diffraction (XRD) technique carried out with the help of Analytical X'Pert - Pro diffractometer (PW 3050/60) in the range $10° < 2\theta < 90°$ at a scanning rate of 1° per minute equipped with a nickel filter using Cu target source (λ = 1.5483 Å). Fig. 1 shows the X-ray diffraction pattern for $(Se_{80}Te_{20})_{90}Ge_6Pb_4$ alloy. All the diffraction peaks can be indexed to the respective JCPDS data ((20.53, 25.28, 26.08, 29.23, 38.23, 41.70, 49.12, 51.72, 60.25, 68.78 and 76.23 corresponding to plane of (111), (100), (100), (200), (213), (220), (311),

(222), (400), (211) and (422) respectively). In addition, the surface morphology and nano-crystalline nature of quaternary alloys is characterized by field emission scanning electron microscope (FESEM). The nano-crystalline nature of each investigated quaternary alloy is further confirmed by FESEM and shows good concordance with X-ray results. It is observed that the crystalline size for quaternary alloys lie in the range between 20 and 80 nm. Fig. 2 (a) - (b) shows some scanned images for $(Se_{80}Te_{20})_{90}$ Ge_6Pb_4 alloy.

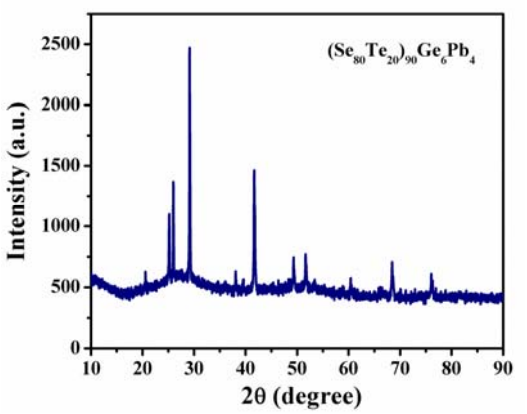

Fig. 1. XRD pattern for chalcogenide $(Se_{80}Te_{20})_{90}Ge_6Pb_4$ alloy

Thin films of the bulk sample were prepared on cleaned glass substrate by thermal evaporation technique at a pressure of 10^{-5} mbar using molybdenum boat. The films were kept inside the deposition chamber for 24 hours to attain the thermodynamic equilibrium. Transmission spectra of $(Se_{80}Te_{20})_{94-x}Ge_6Pb_x$ (x = 0, 2, 4 and 6) in the wavelength range of 500 to 2600 nm studied at room temperature by UV-Vis-NIR spectrophotometer (Perkin Elmer Lambda - 750).

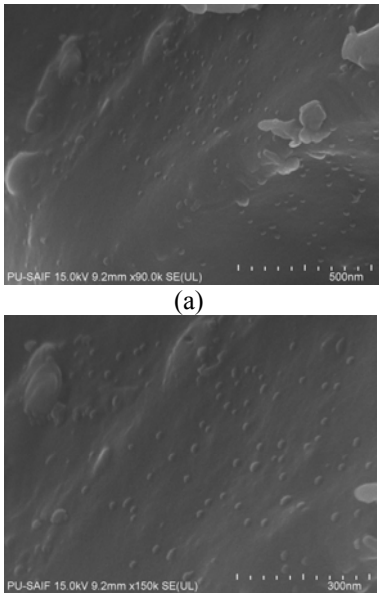

(a)

(b)

Fig. 2. FESEM micrographs of $(Se_{80}Te_{20})_{90}Ge_6Pb_4$ nano-crystalline alloy (a) ×90k, (b) ×150k

3. Results and discussion

In the present work, Swanepoel envelope method was used for the determination of optical constants namely refractive index (n), absorption coefficient (α), extinction coefficient (k) and optical energy gap (E_g) [15]. The advantage of using this method need that the film should be uniformly deposited and have sufficient thickness, only then interference fringes been observed. Fig. 3 shows the transmission spectra for investigated thin films. The transmission maxima and minima in the spectra shows the homogeneity of thin films and also indicates that no optical losses takes place at longer wavelengths [16].

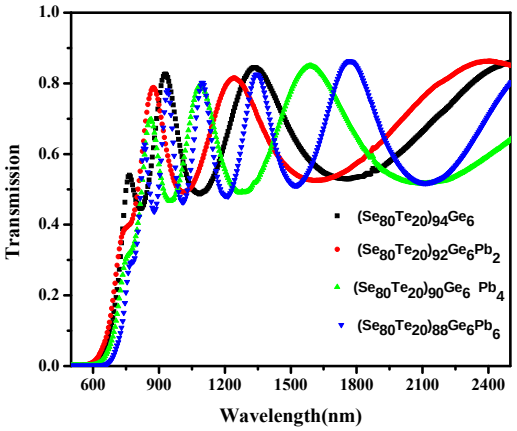

Fig. 3. Transmission spectra of $(Se_{80}Te_{20})_{94-x}Ge_6Pb_x$ (x = 0, 2, 4 and 6) thin films

3.1. Refractive index and film thickness

According to Swanepoel's method, the refractive index of a film is calculated by the following equation:

$$n = [N + (N^2 - s^2)^{1/2}]^{1/2} \quad (1)$$

with

$$N = 2s\frac{(T_M - T_m)}{T_M T_m} + \frac{(s^2+1)}{2} \quad (2)$$

where T_M and T_m are the transmission maxima and the corresponding minima at a certain wavelength (λ) and s is the refractive index of glass substrate (s = 1.51). Refractive index of a material changes under the influence of light. It is the fundamental parameter to find out the optical behavior of a material. The thickness of the film is obtained by the following expression:

$$d = \frac{\lambda_1 \lambda_2}{2(\lambda_2 n_{e1} - \lambda_1 n_{e2})} \quad (3)$$

where n_{e1} and n_{e2} are the refractive indices of the two adjacent maxima or minima at wavelengths λ_1 and λ_2 respectively. The deduced value of film thickness is listed in Table 1 and lies in the range of 471 to 857 nm. The

accuracy of data maybe increased by using the basic equation of interference fringes:

$$2nd = m_o\lambda \quad (4)$$

Here the value of m_0 can be calculated by using the *d* and *n* values in equation (4). Further the accuracy of thickness *d* and refractive index *n* can be improved by taking the corrected m_0 value to an integer or half integer. The refractive index of the sample is found to vary with wavelength (Fig. 4). It is observed that refractive index decreases with the increase in wavelength. The variation of refractive index with wavelength may be attributed to the dispersion of light energy at the different interstitial layers [16]. This shows the normal dispersion in thin films. It is obvious from Table 1 that value of refractive index increases with the increase in Pb content. This may be related to the electronic polarizability. Electronic polarizability is the displacement of electrons with respect to the nuclei with which they are associated upon application of an external electric field. The electronic polarizability of atoms causes the retardation to the electromagnetic waves when propagated through the medium. For the present investigated Se-Te-Ge-Pb system, the atomic radii of Pb, Se, Te are 154 pm, 130 pm, 140 pm respectively [17]. As the atomic radii of lead is more as compare to the replacing selenium and tellurium atoms. The increase of atomic size, increases the polarization i.e. $\alpha = 4\pi\varepsilon_0 r^3$ and which further leads to increase in refractive index. Thus the increase in atomic polarizabilty is leading to increase in refractive index. Cauchy's dispersion relation *i.e.* $n = a + b/\lambda^2$ is used for the extrapolation of n values in order to estimate the refractive index. Where *a, b* are the constants and parameter *a* is called static refractive index (n_o).

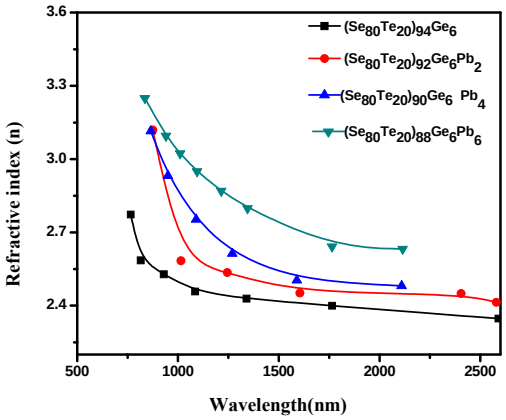

Fig. 4. Variation of refractive index with wavelength for $(Se_{80}Te_{20})_{94-x}Ge_6Pb_x$ (x = 0, 2, 4 and 6) thin films

Table 1. Values of thickness (d), refractive index (n), extinction coefficient (k), optical conductivity (σ), real part (ε_r) , imaginary part (ε_i), optical energy gap (E_g) and cohesive energy (CE) for $(Se_{80}Te_{20})_{94-x}Ge_6Pb_x$ (x = 0, 2, 4 and 6) at 800 nm

Composition	d (nm)	n	k	σ (Sm^{-1})	ε_r	ε_i	E_g (Tauc)	CE (kcal/mol)
$(Se_{80}Te_{20})_{94}Ge_6$	504	2.886	0.0414	4.51×10^{13}	8.34	0.240	1.38	45.00
$(Se_{80}Te_{20})_{92}Ge_6Pb_2$	471	3.291	0.0534	7.31×10^{13}	10.85	0.363	1.34	44.24
$(Se_{80}Te_{20})_{90}Ge_6Pb_4$	564	3.410	0.0685	9.37×10^{13}	11.64	0.479	1.26	43.55
$(Se_{80}Te_{20})_{88}Ge_6Pb_6$	857	3.576	0.0398	5.37×10^{13}	12.82	0.280	1.24	42.83

3.2. Dispersion of refractive index

By using the Wemple-DiDomenico model the dispersion of refractive index may be described by using the single oscillator model. In this W-D model, the refractive index is given by [18]:

$$n^2 = 1 + \frac{E_d E_o}{({E_o}^2 - h\nu^2)} \quad (5)$$

where E_o is single oscillator energy and E_d is the dispersion energy or single oscillator strength. Fig. 5 shows the plot of $(n^2\text{-}1)^{-1}$ versus $(h\nu)^2$ for investigated thin films. For a specific composition, the plot yields a straight line having slope $(E_oE_d)^{-1}$ and intercept on the vertical axis (E_o/E_d) from which one can calculate E_o and E_d directly. Value of static refractive index (n_o) to be derived by extrapolating equation (5) where the value of hν tends to zero. Values of E_o, E_d and n_o are given in Table 2. Value of static refractive index (n_o) obtained by Cauchy's dispersion relation and from WDD model are not found in accord with each other.

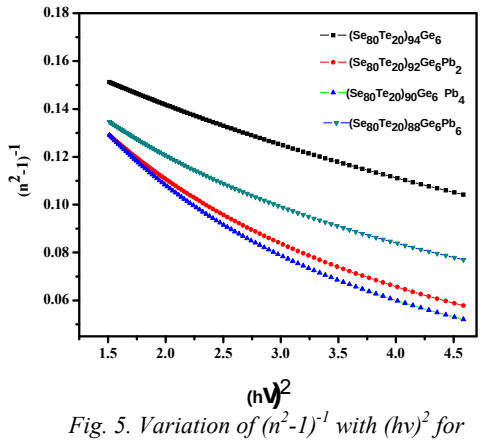

Fig. 5. Variation of $(n^2\text{-}1)^{-1}$ with $(h\nu)^2$ for $(Se_{80}Te_{20})_{94-x}Ge_6Pb_x$ (x = 0, 2, 4 and 6) thin films

Table 2. Values of single-effective oscillator (E_o), dispersion energy (E_d), static refractive index (n_o), for $(Se_{80}Te_{20})_{94-x}Ge_6Pb_x$ (x = 0, 2, 4 and 6)

Composition	E_o	E_d	n_o (Cauchy's)	n_o (WDD)
$(Se_{80}Te_{20})_{94}Ge_6$	3.27	18.74	2.52	2.59
$(Se_{80}Te_{20})_{92}Ge_6Pb_2$	2.51	15.35	2.31	2.66
$(Se_{80}Te_{20})_{90}Ge_6Pb_4$	2.42	14.58	2.20	2.65
$(Se_{80}Te_{20})_{88}Ge_6Pb_6$	2.55	16.41	2.39	2.73

3.3 Absorption coefficient and optical band gap

Optical transmission was strongly dependent on the absorption coefficient. Absorption coefficient (α) explained that how much intensity of the optical beam was reduced when it passes through a particular material. The absorption coefficient is calculated by the expression [14]:

$$\alpha = \frac{1}{d} ln \frac{1}{x} \quad (6)$$

where x is the absorbance. The value of absorption coefficient (α) is found to decrease with the increase in wavelength.

The behavior of absorbance spectra is completely opposite to that of the transmittance spectra.

The optical absorption spectra of a material play an important role to give the basic information about the optical band gap. In chalcogenide glasses, the absorption spectra are divided in to three regions: (1) weak absorption region, which arises due to the defects and disorder in the system. (2) Strong absorption region, which determines the optical energy gap. (3) Absorption edge region, which arises due to disruption of structural and disorder of the system.

In the low absorption region ($\alpha \leq 10^4\ cm^{-1}$), the absorption coefficient shows an exponential dependence on photon energy hv and obeys the Urbach's relation [19]:

$$\alpha = \alpha_o e^{hv/E_e} \quad (7)$$

where α_o is a constant, h is Planck's constant, v is frequency of radiation, and E_e is known as Urbach energy, which is the width of the tail of localized states in the band gap region. E_e represented the degree of disorder and defects in an amorphous semiconductor [20]. The value of E_e could be determined by the plot of ln(α) versus hv.

In the high absorption region ($\alpha \geq 10^4\ cm^{-1}$), the relation between the absorption coefficient and incident photon energy (hv) can be determined by using Tauc relation as follows [21]:

$$(\alpha hv) = \alpha_o (hv - E_g)^n \quad (8)$$

where α_o is a band tailing parameter and it is not dependent on energy. E_g is the optical energy gap, which lies between the localized states near the mobility edges according to the density of states model [22]. Another constant (n) which is called transition mode power factor. The value of n for the direct forbidden, indirect forbidden, direct allowed and indirect allowed are n = 3/2, 3, 1/2, 2 respectively. After plotting the graph between (hv) and $(\alpha hv)^{1/n}$ for all power value of n, the most suitable plot is for n = 2. Therefore now Tauc relation is,

$$(\alpha hv)^{0.5} = \alpha_o (hv - E_g) \quad (9)$$

A direct transition is one in which the maximum energy of valence band edge aligns with the minimum energy level of the conduction band with respect to momentum, whereas in an indirect transition the maximum of valence band energy and minimum of conduction band energy are not aligned with respect to momentum. The variation of $(\alpha hv)^{0.5}$ with photon energy (hv) for the prepared thin films of $(Se_{80}Te_{20})_{94-x}Ge_6Pb_x$ (x = 0, 2, 4 and 6) is shown in Fig. 6. The values of optical band gap are taken as the intercept of $(\alpha hv)^{0.5}$ vs (hv) at $(\alpha hv)^{0.5} = 0$. The values of optical band gap are listed in Table 1.

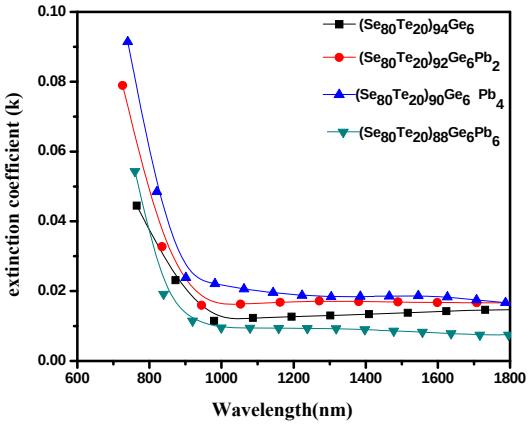

Fig. 6. Plot of extinction coefficient (k) versus wavelength for $(Se_{80}Te_{20})_{94-x}Ge_6Pb_x$ (x = 0, 2, 4 and 6) thin films

Optical band gap is closely related to the energy difference between the top of valence band and bottom of conduction band. Chalcogenide always contains a high concentration of unsaturated bonds and these defects were responsible for the high concentration of localized states in the band gap. Decrease in band gap value with increasing lead content changes the bond length/bond angle and this caused an increase in defect of states due to which there was decrease in band gap [23]. Energy band gap was also correlated with the heat of atomization, the latter being cohesive energy as they represents the relative bond strength. Theoretically calculated H_s value for $(Se_{80}Te_{20})_{94-x}Ge_6Pb_x$ (x = 0, 2, 4 and 6) are 230.36kJ/mol, 229.84kJ/mol, 229.32kJ/mol and 228.80 kJ/mol respectively [24]. Since optical band gap was a bond sensitive property, decrease in mean bond energy i.e. 2.016 eV/atom, 2.004 eV/atom, 1.995 eV/atom, 1.990 eV/atom with Pb results the decrease in optical band gap [14]. Addition of lead to Se-Te-Ge system caused a decrease in cohesive energy, which leads to decrease in conduction band edge. This further caused a decrease in gap between bonding and anti-bonding orbitals i.e. decrease in energy gap. Decrease in optical energy gap is also related with electronegativity of elements. The valence band of chalcogenide glasses have lone pair p-orbital. These lone pair electrons have higher energy than electronegative atoms (i.e. near to electropositive atoms). The introduction of electropositive element to the composite, the energy of lone pair gets increased and as a result the valence band move towards the energy gap [25].

3.4. Extinction coefficient

The optical behavior of a material is used to govern its extinction coefficient. Extinction coefficient (k) shows the amount of absorption loss when electromagnetic wave propagated through material and is calculated by:

$$k = \frac{\alpha\lambda}{4} \tag{10}$$

From Fig. 7, it is clear that extinction coefficient *(k)* decreases with the increase in wavelength for the prepared thin films. The change in absorption coefficient is due to the variation of absorption, fall in extinction coefficient is due to the absorption of light at the grain boundaries. The reduction of extinction coefficient shows that the material is becoming transparent with wavelength which is useful for optical materials in the high wavelength region. Value of extinction coefficient increases with the increase in lead concentration as this behavior of k is related directly to the absorption of light. The value of k decreases slightly for 6% of lead, this is due to the greater thickness as compared to other films because it has inverse relation with absorption [26]. The reduction in extinction coefficient value with composition for the prepared thin films is listed in Table 1.

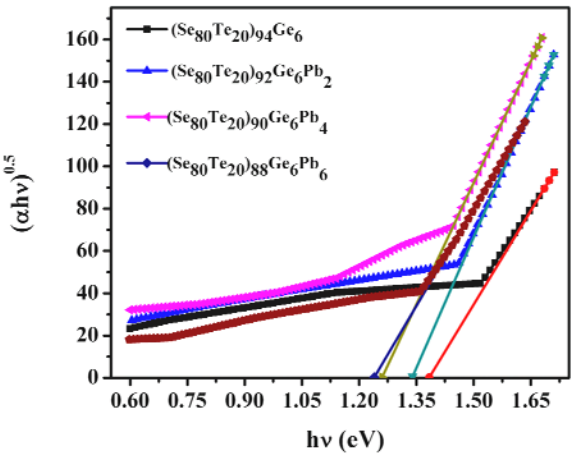

Fig. 7. Plot of $(\alpha h\nu)^{0.5}$ versus $(h\nu)$ for $(Se_{80}Te_{20})_{94-x}Ge_6Pb_x$ (x = 0, 2, 4 and 6) thin films

3.5. Dielectric constant and optical conductivity

Dielectric constant was the intrinsic property of a material. The real and imaginary part of the dielectric constant of thin film could be estimated by using the values of n and k in the following relations [23]:

$$\varepsilon_r = n^2 - k^2 \tag{11}$$

and

$$\varepsilon_i = 2nk \tag{12}$$

Real part of dielectric constant gave the retardation of velocity of light and imaginary part told about the absorption loss of light due to polarization, when propagating through the material medium. The real and imaginary part of dielectric constant followed the same trend as that of refractive index and extinction coefficient. Optical conductivity *(σ)* which was an important parameter for the practical application could be calculated as [27]:

$$\sigma = \frac{\alpha nc}{4} \tag{13}$$

where *α, n* and *c* were the absorption coefficient, refractive index and velocity of light respectively.

Fig. 8 shows the variation of optical conductivity with *(hν)* and from where we could observe that optical conductivity increases with the photon energy. Value of refractive index *(n),* extinction coefficient *(k),* optical conductivity *(σ),* real part *(ε_r),* imaginary part *(ε_i)* for $(Se_{80}Te_{20})_{94-x}Ge_6Pb_x$ (x = 0, 2, 4 and 6) were given in table1 and found to be consistent as obtained for other chalcogenide glasses [23, 27] .

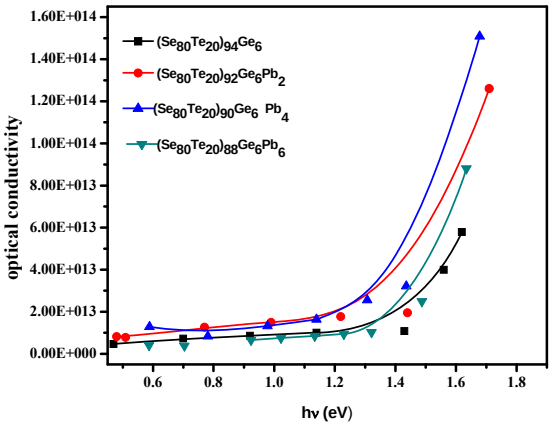

Fig. 8. Plot of optical conductivity (σ) versus (hv) for $(Se_{80}Te_{20})_{94-x}Ge_6Pb_x$ (x = 0, 2, 4 and 6) thin films

4. Conclusions

The optical characterization of quaternary $(Se_{80}Te_{20})_{94-x}Ge_6Pb_x$ (x = 0, 2, 4 and 6) thin films is made in the wavelength range (500 – 2600 nm) using transmission spectra. The value of refractive index *(n)* and extinction coefficient *(k)* also decreases with wavelength, this shows that absorption losses decrease and the material is becoming transparent with higher wavelength. The refractive index and extinction coefficient increases with the increase in lead (Pb) concentration. The real and imaginary part of the dielectric constant acts similarly as the refractive index and extinction coefficient behave respectively. Optical energy gap decreases with the lead concentration and has been explained on the basis of heat of atomization and mean bond energies. Also lead is metallic in nature so addition of it to the system decreases the band gap.

References

[1] M. Kruncks, A. Katerski, T. Dedova, I. Oja Acik, A. Mere, Sol. Energy Mater. Sol. Cells **92,** 1016 (2008).
[2] A. L. Briseno, S. C. B. Mannsfeld, X. Lu, Y. Xiong, S. A. Jenekhe, Z. Bao, Y. Xia, Nano Lett. **7**, 688 (2007).
[3] B. L. Allen, P. D. Kichambare, A. Star, Adv. Mater. **19**, 1439 (2007).
[4] M. A. M. Khan, W. K. Khan, Mansour Alhoshan, M. S. Alsalhi, Aldwayyan, M. Zulfequar, J. Alloys Compd. **503,** 397 (2010).
[5] B. Molina Concha, E. De Biasi, R. D. Zysler, Physica B **403,** 390 (2008).
[6] I. Na. Chao, P. J. McCann, W. L. Yuan, S. Yuan, Thin Solid Films **323,** 126 (1998).
[7] B. S. Patial, N. Thakur, S. K. Tripathi, Thermochim. Acta **513**, 1 (2011).
[8] J. Troles, Y. Niu, C. Duverger-Arfuso, F. Smektala, L. Brillard, V. Nazabal, V. Moizan, F. Desevedavy, P. Houizot, Mater. Res. Bull. **43,** 976 (2008).
[9] F. J. Meca, M. M. Quintas, F. J. R. Sanchez, Sensors Actuators **84,** 45 (2000).
[10] M. M. Ibrahim, S. A. Saleh, E. M. M. Ibrahim, A. M. Abdel Hakeem, J. Alloys Compd. **452,** 200 (2008).
[11] Q. Li, Y. Ding, M. Shao, J. Wu, G. Yu,Y. Qian, Mater. Res. Bull. **38,** 539 (2003).
[12] R. N. Bhattacharya, J. Appl. Electrochem. Soc. **16,** 168 (1986).
[13] S. A. Khan, F. A. Al-Agel, A. A. Al-Ghamdi, Superlattices and Microstructures. **47,** 695 (2010).
[14] Mainika, P. Sharma, S. C. Katyal, N. Thakur, J. Phys. D. **41,** 235301 (2008).
[15] R. Swanepoel, J. Phys. E: Sci. Instrum. **16,** 1214 (1983).
[16] G. A. N. Connell, Optical properties of amorphous Semiconductors, Springer, Berlin, Heidelberg (1985).
[17] A. Dashan, Optical Materials **32,** 247 (2009).
[18] S. H. Wemple, M. DiDomenico, Phys. Rev. B **3** 1338 (1971).
[19] F. Urbach, Phys. Rev. B **92,** 1324 (1953).
[20] V. Pamukchieva, A. Szekeres, K. Todorova, E. Svab, M. Fabian, Optical Materials **32**, 45 (2009).
[21] J. Tauc, The Optical properties of Semiconductors (Amsterdam: North – Holland) (1970).
[22] M. I. Abd- Elrahman, M. M. Hafiz, A. M. Abdelraheem, A. A. Abu-Sehly, Optical materials **50**, 99 (2015).
[23] N. Sharma, S. Sharma, A. Sarin R. Kumar, Optical Materials **51,** 56 (2016).
[24] N. Sharma, B. S. Patial, N. Thakur, Ind. J. Pure Appl. Phys. **56**, 128 (2018).
[25] E. R. Shaaban, H. A. Elshaikh, M. M. Soraya, Optoelectron. Adv. Mat. **9**(5-6), 587 (2015).
[26] C. Das, J. Begam, T. Begam, S. Choudhary, Journal of Bangladesh Academy of Sciences **37**, 83 (2013).
[27] A. K. Singh, N. Mehta, K. Singh, Physica B **404**, 3470 (2009).

*Corresponding author: bspatial@gmail.com